

# Ionic Hydrogen Bond Effects on the Acidities, Basicities, Solvation, Solvent Bridging, and Self-Assembly of Carboxylic Groups

Michael Meot-Ner (Mautner),\*<sup>†</sup> Donald E. Elmore,<sup>‡,§</sup> and Steve Scheiner<sup>‡</sup>

Contribution from the Department of Chemistry, University of Canterbury, Christchurch 8001, New Zealand, Department of Chemistry, Virginia Commonwealth University, Richmond, Virginia 23284-2006, and Department of Chemistry and Biochemistry, Southern Illinois University, Carbondale, Illinois 62901-4409

Received June 22, 1998

**Abstract:** Ionic assemblies of acetic acid and water form unlimited hydrogen bond networks. The stabilities of the networks correlate with the intrinsic acidities of the components, leading to strong  $\text{CH}_3\text{COO}^- \cdots \text{HOOCCH}_3$  bonds and weak  $\text{CH}_3\text{COO}^- \cdots \text{H}_2\text{O}$  bonds. These relations apply from strong bonds in small aggregates to weak bonds in large assemblies, and affect the energies of acid dissociation and self-assembly. Partial solvation of  $\text{CH}_3\text{COO}^-$  by four  $\text{H}_2\text{O}$  molecules facilitates acid dissociation and decreases the  $\text{CH}_3\text{COO}^- - \text{H}^+$  bond dissociation energy by 332 kJ/mol (80 kcal/mol). The stabilities of the hydrogen bond networks increase with  $\text{CH}_3\text{COOH}$  content, and aggregation decreases further the acid dissociation energy by forming strong  $\text{CH}_3\text{COO}^- \cdots \text{HOOCCH}_3$  bonds about the ions and by stabilizing the released protons in  $(\text{CH}_3\text{COOH})_m(\text{H}_2\text{O})_n\text{H}^+$  assemblies. The combination of strong  $\text{CH}_3\text{COO}^- \cdots \text{HOOCCH}_3$  bonds and weak  $\text{CH}_3\text{COO}^- \cdots \text{H}_2\text{O}$  bonds makes self-assembly with solvent displacement particularly favorable for carboxylic acids, explaining their assembly in bilayers and membranes. Ab initio calculations show that isomeric assemblies with directly bonded and solvent-bridged structures have similar energies. As well, the solvent-bridged species  $\text{CH}_3\text{COO}^- \cdots \text{H}_2\text{O} \cdots \text{HOOCCH}_3$  has similar energy to its cation-bridged isomer  $\text{CH}_3\text{COO}^- \cdots \text{H}_3\text{O}^+ \cdots \text{OOCCH}_3$ . In this transition state the adjacent anions stabilize the central cation, providing low-energy pathways for proton transfer between carboxylic groups.

## Introduction

The thermochemistry of acid and base dissociation is affected strongly by the solvation of the resulting ions, including strong hydrogen bonding in the inner solvent shells. Ionic hydrogen bonds in the inner shells can be modeled by gas-phase clusters,<sup>1,2</sup> and comparison with bulk solvation energies can quantify other solvation factors such as the dielectric, cavity-forming, and hydrophobic solvation terms.<sup>3</sup> A significant finding is that the hydrogen bond strengths correlate inversely with the relative acidities and basicities of the components.<sup>1–6</sup> These relations have critical effects on the stabilities of mixed assemblies, on ion solvation, on acid and base dissociation, and on ionic aggregation including self-assembly into bilayers and membranes.

Clustering data can also model ion–solvent interactions in biological assemblies, where ionized carboxylate groups interact with solvent molecules and with neutral carboxylic groups. For example, in previous work we measured interaction energies

of the acetate ion with several functional molecules<sup>4,5</sup> and used these data to model ionic hydrogen bonds in serine protease enzymes.<sup>6</sup>

The dissociation of carboxylic groups such as that of acetic acid in water and in biological environments yields  $\text{RCOO}^-$  anions, here modeled by  $\text{CH}_3\text{COO}^-$  (denoted as  $\text{Ac}^-$ ) and  $\text{H}_3\text{O}^+$  (denoted as  $\text{WH}^+$ ) or  $(\text{CH}_3\text{COOH})\text{H}^+$  (denoted as  $(\text{AcH})\text{H}^+$ ) cations. In dilute solutions these species are solvated by  $\text{H}_2\text{O}$  molecules (W), but in concentrated solutions and in biological environments, the ions can also interact with further  $\text{RCOOH}$  groups to form hydrogen-bonded networks. The stabilities of ionic hydrogen bond networks in mixed clusters were investigated in  $\text{CH}_3\text{CN}/\text{H}_2\text{O}$ ,  $(\text{CH}_3)_2\text{O}/\text{CH}_3\text{OH}$ ,  $\text{NH}_3/\text{H}_2\text{O}$ , and  $\text{CH}_3\text{OH}/\text{H}_2\text{O}$  mixtures,<sup>7–10</sup> where ionic hydrogen bond networks contribute up to 190 kJ/mol (45 kcal/mol) to the solvation enthalpies of ions.<sup>3</sup> Similarly, the mixed clusters of  $\text{CH}_3\text{COOH}/\text{H}_2\text{O}$  should also allow strongly stabilizing ionic hydrogen bond networks.

In the present work we investigate the thermochemistry and ab initio structures of acetic acid/water aggregates, compare cationic and anionic hydrogen bond networks, and examine the mutual effects of partial solvation, acidity, basicity, and self-assembly.

## Experimental and Computational Methods

The experiments were performed using a pulsed high-pressure mass spectrometer.<sup>11</sup> Reactant mixtures contained  $\text{CH}_4$  or  $\text{N}_2$  as the carrier

\* To whom correspondence should be addressed at the University of Canterbury. E-mail: m.mautner@chem.canterbury.ac.nz.

<sup>†</sup> University of Canterbury and Virginia Commonwealth University.

<sup>‡</sup> Southern Illinois University.

<sup>§</sup> Present address: Department of Chemistry, California Institute of Technology, Pasadena, California 91125.

(1) Kebarle, P. *Annu. Rev. Phys. Chem.* **1977**, *28*, 445; Meot-Ner (Mautner), M. *J. Am. Chem. Soc.* **1984**, *106*, 1257 and 1265.

(2) Castleman, A. W.; Keese, R. G. *Chem. Rev.* **1986**, *86*, 589; Meot-Ner (Mautner), M.; Speller, C. V. *J. Phys. Chem.* **1986**, *90*, 6616; Hiraoka, K.; Takimoto, H.; Morise, K. *J. Am. Chem. Soc.* **1986**, *108*, 5683; Hiraoka, K. *Bull. Chem. Soc. Jpn.* **1987**, *60*, 2555.

(3) Meot-Ner (Mautner), M. *J. Phys. Chem.* **1987**, *91*, 417.

(4) Meot-Ner (Mautner), M.; Sieck, L. W. *J. Am. Chem. Soc.* **1986**, *108*, 7525.

(5) Meot-Ner (Mautner), M. *J. Am. Chem. Soc.* **1988**, *110*, 3854.

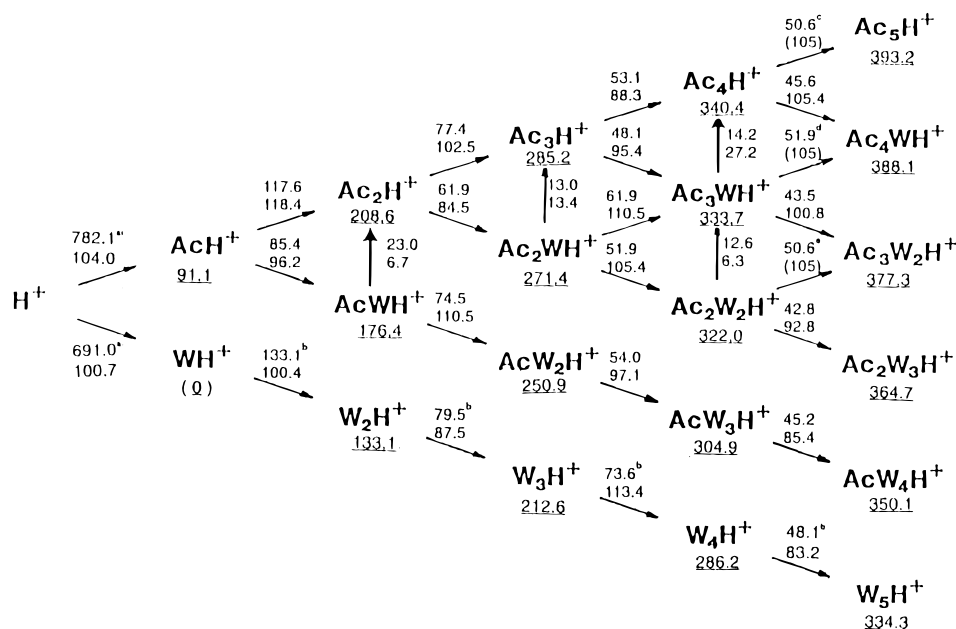
(6) Meot-Ner (Mautner), M. *J. Am. Chem. Soc.* **1988**, *110*, 3075.

(7) Deakyne, C. A.; Meot-Ner (Mautner), M.; Campbell, C. L.; Hughes, M. G.; Murphy, S. P. *J. Chem. Phys.* **1986**, *90*, 4648.

(8) Grimsrud, E. P.; Kebarle, P. *J. Am. Chem. Soc.* **1973**, *95*, 7939.

(9) Payzant, J. D.; Cunningham, A. J.; Kebarle, P. *Can. J. Chem.* **1973**, *51*, 3242.

(10) Meot-Ner (Mautner), M. *J. Am. Chem. Soc.* **1986**, *108*, 6189.

**Scheme 1.** Thermochemistry of Protonated Acetic Acid and Water Clusters<sup>a</sup>

<sup>a</sup> Note shorthand notation in Scheme 1, Ac = CH<sub>3</sub>COOH, W = H<sub>2</sub>O, AcH<sup>+</sup> = (CH<sub>3</sub>COOH)H<sup>+</sup>, Ac<sub>n</sub>H<sup>+</sup> = (CH<sub>3</sub>COOH)<sub>n</sub>H<sup>+</sup>. Values of  $-\Delta H^\circ$  (kJ/mol), top number, and  $-\Delta S^\circ$  (J/mol K), bottom number, over arrows. Numbers under formulas indicate the enthalpy of dissociation to H<sub>2</sub>O<sup>+</sup> and neutrals. Protonation thermochemistry from NIST database (ref 22). Values for AcW<sub>n-1</sub>H<sup>+</sup> → AcW<sub>n</sub>H<sup>+</sup> from ref 26, except AcH<sup>+</sup> → AcWH<sup>+</sup> from the present results, which may be compared with  $-\Delta H^\circ = 84.1$  kJ/mol and  $-\Delta S^\circ = 87.9$  J/mol K from ref 26. <sup>b</sup> From ref 26. <sup>c-e</sup>  $\Delta S^\circ$  values in parentheses are estimated, and corresponding  $\Delta H^\circ$  values are derived from experimental values as follows ( $-\Delta G^\circ$ (kJ/mol),  $T$  (K)): (c) Ac<sub>3</sub>H<sup>+</sup> → Ac<sub>4</sub>H<sup>+</sup>, 24.3, 255; (d) Ac<sub>3</sub>WH<sup>+</sup> → Ac<sub>4</sub>WH<sup>+</sup>, 25.5, 251; (e) Ac<sub>2</sub>W<sub>2</sub>H<sup>+</sup> → Ac<sub>3</sub>W<sub>2</sub>H<sup>+</sup>, 24.3, 255. Uncertainty estimates for  $\Delta H^\circ$  (kJ/mol) and for  $\Delta S^\circ$  (J/mol K): AcH<sup>+</sup> → AcWH<sup>+</sup>, 4.3, 8.7; AcH<sup>+</sup> → Ac<sub>2</sub>H<sup>+</sup>, 6.5, 13.2; Ac<sub>2</sub>H<sup>+</sup> → Ac<sub>2</sub>WH<sup>+</sup>, 5.3, 15.2; Ac<sub>2</sub>H<sup>+</sup> → Ac<sub>3</sub>H<sup>+</sup>, 3.3, 9.7; Ac<sub>2</sub>WH<sup>+</sup> → Ac<sub>3</sub>H<sup>+</sup>, 5.2, 16.0; Ac<sub>2</sub>WH<sup>+</sup> → Ac<sub>2</sub>W<sub>2</sub>H<sup>+</sup>, 2.6, 9.5; Ac<sub>2</sub>WH<sup>+</sup> → Ac<sub>3</sub>WH<sup>+</sup>, 2.5, 8.8; Ac<sub>3</sub>H<sup>+</sup> → Ac<sub>3</sub>WH<sup>+</sup>, 4.2, 15.7; Ac<sub>3</sub>H<sup>+</sup> → Ac<sub>4</sub>H<sup>+</sup>, 2.4, 9.2; Ac<sub>2</sub>W<sub>2</sub>H<sup>+</sup> → Ac<sub>3</sub>WH<sup>+</sup>, 3.4, 12.2; Ac<sub>3</sub>WH<sup>+</sup> → Ac<sub>4</sub>H<sup>+</sup>, 3.9, 14.8; Ac<sub>2</sub>W<sub>2</sub>H<sup>+</sup> → Ac<sub>2</sub>W<sub>3</sub>H<sup>+</sup>, 5.4, 20.8; Ac<sub>3</sub>WH<sup>+</sup> → Ac<sub>3</sub>W<sub>2</sub>H<sup>+</sup>, 2.7, 10.6; Ac<sub>4</sub>H<sup>+</sup> → Ac<sub>4</sub>WH<sup>+</sup>, 3.2, 13.3. Uncertainty estimates for  $\Delta H^\circ$  and  $\Delta S^\circ$  values are evaluated from  $u = 2(\sum\sigma^2/n)^{1/2}$ , where  $\sigma$  values are the standard deviations of the  $\Delta H^\circ$  and  $\Delta S^\circ$  values from each van't Hoff plot,  $n$  the number of replicate van't Hoff plots obtained for each equilibrium, usually 2–4, and the multiplier 2 is a conventional coverage factor (B. N. Taylor and C. E. Kuyatt, NIST Technical Note 1297, *Guidelines for Evaluating the Uncertainty of NIST Measurement Results*; US Government Printing Office: Washington, 1994). For  $\Delta G^\circ$  measurements at a single temperature, the uncertainty estimate is  $\pm 0.8$  kJ/mol.

gas and 0.01–1% H<sub>2</sub>O and CH<sub>3</sub>COOH (in some cases CD<sub>3</sub>COOH) vapor. To generate anions, we also added trace amounts of the electron capture agent CH<sub>3</sub>ONO, prepared by the method of Bartmess,<sup>12</sup> The mixtures were prepared in a 3 L bulb heated to 150–180 °C and were allowed to flow to the ion source through stainless steel lines heated to similar temperatures. The mixtures were ionized using 0.7–1 ms pulses of 700–1000 eV electrons. Relative ion concentrations were observed to 2–4 ms after the pulse. Relative equilibrium concentrations of the cluster ions were obtained after sufficiently long reaction times to achieve constant ion ratios, which usually occurred during the ionizing pulse.

Equilibrium constants for the addition of CH<sub>3</sub>COOH molecules, reaction 1, are calculated from eq 2 and analogous equations for the anions, where [BH<sup>+</sup>(CH<sub>3</sub>COOH)] and [BH<sup>+</sup>] are the respective ion concentrations or partial pressures in the source and  $P$  is the partial pressure of CH<sub>3</sub>COOH vapor.



$$K_1 = [\text{BH}^+(\text{CH}_3\text{COOH})]/([\text{BH}^+]P) \quad (2)$$

A potential source of error is that acetic acid can dimerize in the gas phase,<sup>13</sup> as in eq 3.



(11) Meot-Ner (Mautner), M.; Sieck, L. W. *J. Am. Chem. Soc.* **1991**, *113*, 4448.

(12) Bartmess, J. E.; Scott, J. A.; McIver, R. T. *J. Am. Chem. Soc.* **1979**, *101*, 6046.

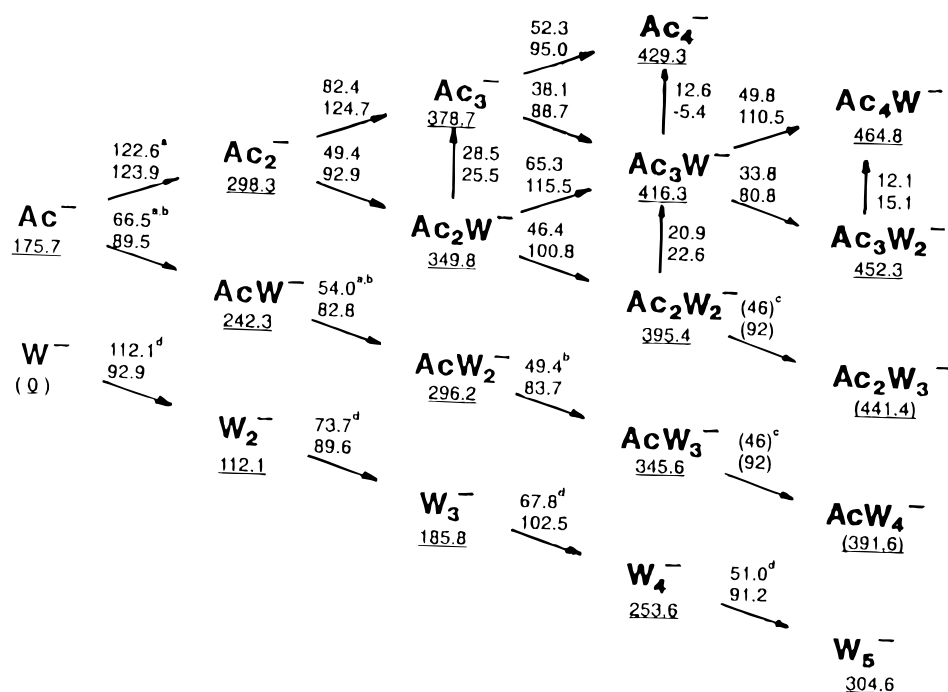
If a fraction  $\alpha$  of the CH<sub>3</sub>COOH introduced vapor is in dimers, the nominal pressure calculated from the mixture composition should be corrected to  $P = (1 - \alpha)P_{\text{nominal}}$  for use in eq 2.

To evaluate if equilibrium (3) introduces significant errors, we note that literature values for reaction 3 are  $\Delta H^\circ_3 = -63.2$  kJ/mol ( $-15.1$  kcal/mol) and  $\Delta S^\circ_3 = -149.4$  J mol<sup>-1</sup> K<sup>-1</sup> ( $-35.7$  cal mol<sup>-1</sup> K<sup>-1</sup>)<sup>13b</sup> or  $\Delta H^\circ_3 = -69.9$  kJ/mol ( $-16.7$  kcal/mol) and  $\Delta S^\circ_3 = -176.2$  J mol<sup>-1</sup> K<sup>-1</sup> ( $-42.1$  cal mol<sup>-1</sup> K<sup>-1</sup>)<sup>13c</sup>. In our experiments, the highest value of  $P(\text{AcH})$  is  $6.5 \times 10^{-7}$  bar. As calculated from the thermochemistry, under these conditions the monomer partial pressure decreases by 2% at 270 K, 4% at 260 K, and 12% at 250 K due to the formation of neutral (AcH)<sub>2</sub> dimers. Even the largest value, at the lowest temperature, would decrease  $\ln K_1$  by a factor of 0.12, about the uncertainty of  $\ln K$  determinations. The neutral dimerization effects are therefore insignificant above 250 K where the measurements for AcH addition reactions were performed.

To avoid this problem altogether in mixed clusters, we measured the mixed clusters mostly through H<sub>2</sub>O addition equilibria to (AcH)<sub>n</sub>H<sup>+</sup> and Ac<sup>-</sup>(AcH)<sub>n</sub> clusters, where the value of  $K = [(\text{AcH})_n\text{H}^+(\text{H}_2\text{O})_n]/[(\text{AcH})_n\text{H}^+(\text{H}_2\text{O})_{n-1}]P(\text{H}_2\text{O})$  is not affected by  $P(\text{AcH})$  and therefore not affected by the dimerization of the acid.

Neutral dimerization appears to have affected only the highest accessible clustering reaction of AcH which yielded unexpectedly large apparent  $-\Delta H^\circ$  and  $-\Delta S^\circ$  values. The van't Hoff plots measured for (AcH)<sub>4</sub>H<sup>+</sup> + Ac → (AcH)<sub>5</sub>H<sup>+</sup> between 230 and 260 K yielded  $\Delta H^\circ$  values of  $-54$  to  $-63$  kJ/mol ( $-13$  to  $-15$  kcal/mol) and  $\Delta S^\circ$  from  $-117$  to  $-134$  J mol<sup>-1</sup> K<sup>-1</sup> ( $-28$  to  $-32$  cal mol<sup>-1</sup> K<sup>-1</sup>), larger than

(13) (a) Frurip, D. J.; Curtiss, L. A.; Blander, M. *J. Am. Chem. Soc.* **1980**, *102*, 2610. (b) Curtiss, L. A.; Frurip, D. J.; Blander, M. *J. Phys. Chem.* **1982**, *86*, 1120. (c) Mikhailova, O. K.; Solomentseva, T. V.; Markuzin, N. P. *VINITI*; Deposited Document 1999-81, 1981.

**Scheme 2.** Thermochemistry of Acetate/Acetic Acid/Water Clusters<sup>a</sup>

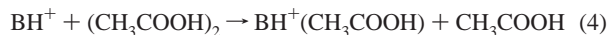
<sup>a</sup> Note shorthand notation in Table 2,  $\text{Ac}_n^- = \text{CH}_3\text{COO}^-(\text{CH}_3\text{COOH})_{n-1}$ ,  $\text{W}_n^- = \text{OH}^-(\text{H}_2\text{O})_{n-1}$ . Values of  $-\Delta H^\circ$  (kJ/mol), top number, and  $-\Delta S^\circ$  (J/mol K), bottom number, over arrows. Numbers under formulas indicate enthalpy of dissociation to  $\text{OH}^-$  and neutrals. Deprotonation enthalpy difference between  $\text{H}_2\text{O}$  and  $\text{CH}_3\text{COOH}$  from ref 22. Values for  $\text{Ac}^- \rightarrow \text{Ac}_2^-$  from ref 4. <sup>b</sup> For  $\text{Ac}^- \rightarrow \text{AcW}^- \rightarrow \text{AcW}_2^-$ , average values from refs 4 and 5,  $\text{AcW}_2^- \rightarrow \text{AcW}_3^-$  from ref 5. <sup>c</sup> Estimated values from usual trend of approach to neutral condensation thermochemistry, ref 26. <sup>d</sup> From ref 5. Uncertainty estimates for  $\Delta H^\circ$  (kJ/mol) and for  $\Delta S^\circ$  (J/mol K) are the following:  $\text{Ac}_2^- \rightarrow \text{Ac}_2\text{W}^-$ , 2.8, 8.7;  $\text{Ac}_2^- \rightarrow \text{Ac}_3^-$ , 2.3, 6.7;  $\text{Ac}_2\text{W}^-$ ,  $\text{Ac}_3^-$ , 4.9, 15.8;  $\text{Ac}_2\text{W}^- \rightarrow \text{Ac}_2\text{W}_2^-$ , 2.4, 8.8;  $\text{Ac}_2\text{W}^- \rightarrow \text{Ac}_3\text{W}^-$ , 2.4, 8.7;  $\text{Ac}_2\text{W}^- \rightarrow \text{Ac}_3\text{W}^-$ , 4.0, 14.4;  $\text{Ac}_3^- \rightarrow \text{Ac}_3\text{W}^-$ , 1.7, 6.1;  $\text{Ac}_3^- \rightarrow \text{Ac}_4^-$ , 2.6, 9.6;  $\text{Ac}_3\text{W}^- \rightarrow \text{Ac}_3\text{W}_2^-$ , 0.3, 1.1;  $\text{Ac}_3\text{W}^- \rightarrow \text{Ac}_4^-$ , 0.4, 1.7;  $\text{Ac}_3\text{W}^- \rightarrow \text{Ac}_4^-$ , 2.4, 9.9;  $\text{Ac}_3\text{W}_2^- \rightarrow \text{Ac}_4\text{W}^-$ , 2.6, 10.8;  $\text{Ac}_2\text{W}_2^- \rightarrow \text{Ac}_3\text{W}^-$ , 4.3, 9.6;  $\text{Ac}_3\text{W}^- \rightarrow \text{Ac}_4^-$ , 1.7, 7.5;  $\text{Ac}_3\text{W}^- \rightarrow \text{Ac}_3\text{W}_2^-$ , 0.8, 4.2;  $\text{Ac}_3\text{W}^- \rightarrow \text{Ac}_4\text{W}^-$ , 10.0, 48.2;  $\text{Ac}_3\text{W}_2^- \rightarrow \text{Ac}_4\text{W}^-$ , 10.9, 22.6. For derivation of uncertainty estimates, see footnotes to Scheme 1. For  $\Delta G^\circ$  measurements at a single temperature, the uncertainty estimate is 0.8 kJ/mol.

for the preceding clustering step, which would be unusual. Therefore, we report  $\Delta H^\circ$  for this reaction as derived from  $\Delta G^\circ$  measured at the highest observable temperature, 257 K, where neutral clustering should be minimal, using an estimated  $\Delta S^\circ$  value.

Because of the uncertainty in this reaction, the preceding step  $(\text{AcH})_3\text{H}^+ + \text{AcH} \rightarrow (\text{AcH})_4\text{H}^+$  was examined by varying the partial pressure of AcH over the widest usable range and in two carrier gases,  $\text{N}_2$  and  $\text{CH}_4$ , and gave the following results ( $P(\text{CH}_3\text{COOH})$  (mbar),  $-\Delta H^\circ$  (kJ/mol) (kcal/mol),  $-\Delta S^\circ$  (J mol<sup>-1</sup> K<sup>-1</sup>) (cal mol<sup>-1</sup> K<sup>-1</sup>): 0.00024, 54.8 (13.1), 91.2 (21.8); 0.00053, 51.0 (12.2), 82.8 (19.8); 0.00087, 54.8 (13.1), 96.7 (23.1); 0.0013, 51.5 (12.3), 82.8 (19.8). Similarly, as is our standard practice, the equilibrium constants for all of the reported reactions were replicated with the values of  $P(\text{H}_2\text{O})$  and  $P(\text{CH}_3\text{COOH})$  varied by factors 2–10. In all cases, the equilibrium constant was independent of partial pressure. These tests show that the problem experienced for the highest cluster did not affect the other measurements at higher temperatures where neutral dimerization and condensation are not significant.

The estimated uncertainties in the footnotes of Schemes 1 and 2 are significant for some of the large clusters. The uncertainty in  $\Delta H^\circ$  is affected by the small temperature range where some of the higher clusters are observable. The uncertainty in  $\Delta S^\circ$  is affected by the uncertainties in the absolute value of the vapor pressure of the polar and strongly adsorbing  $\text{CH}_3\text{COOH}$  component in the ion source. This uncertainty affects only  $\Delta S^\circ$  as  $P(\text{CH}_3\text{COOH})$  is usually constant during a temperature study. Finally, our uncertainty estimates are derived by multiplying the standard deviations of replicate measurements by a conservative multiplier factor of 2 following NIST procedures (see the footnotes to Scheme 1), whereas in most reports only the smaller uncorrected standard deviations are used.

Note that, in the presence of neutral dimers, switching equilibria (4) can also occur.



However, if all the reactions are at equilibrium, this will not introduce an error into the measurement of  $K_1$ .

The ab initio calculations were carried out using the Gaussian-92 code.<sup>14</sup> All geometries were optimized at the SCF/4-31G level.<sup>15</sup> This basis set was chosen for computational efficiency, which allowed a thorough search of the conformational space of the each complex. Complexation energies computed at this level are generally accurate for ionic complexes, which are dominated by electrostatic interactions.<sup>16–18</sup> Another advantage of the 4-31G basis set at the SCF level is that the proton transfer barriers are typically quite similar to those obtained with larger sets and with correlation added.<sup>19,20</sup> Minima reported below were tested for stability in terms of proton transfer across hydrogen bonds. In other words, transfer potentials were examined to ascertain that they contained only one minimum, rather than two. Higher level calculations were performed at the geometries obtained at the SCF/4-31G level. MP2/6-31+G\* calculations include electron correlation via second-order Moller–Plesset perturbation theory, and the larger basis set includes polarization and diffuse functions on nonhydrogen atoms.

## Results and Discussion

**1. The Structures of the Dimers.** Van't Hoff plots for the various equilibria are shown in Figures 1–4. The results are summarized in Schemes 1 and 2.

(14) Frisch, M. J.; et al. In *Gaussian, Inc.*; Pittsburgh PA, 1993.

(15) Ditchfield, R.; Hehre, W. J.; Pople, J. A. *J. Chem. Phys.* **1971**, *54*, 724.

(16) Rohlfing, C. M.; Allen, L. C.; Cook, C. M.; Schlegel, H. B. *J. Chem. Phys.* **1983**, *78*, 2498.

(17) Desmeules, P. J.; Allen, L. C. *J. Chem. Phys.* **1980**, *72*, 4731.

(18) Scheiner, S.; Harding, L. B. *J. Am. Chem. Soc.* **1981**, *103*, 2169.

(19) Scheiner, S. *Acc. Chem. Res.* **1985**, *18*, 174.

(20) Scheiner, S.; Szczesniak, M. M.; Bigham, L. D. *Int. J. Quantum Chem.* **1983**, *23*, 739.

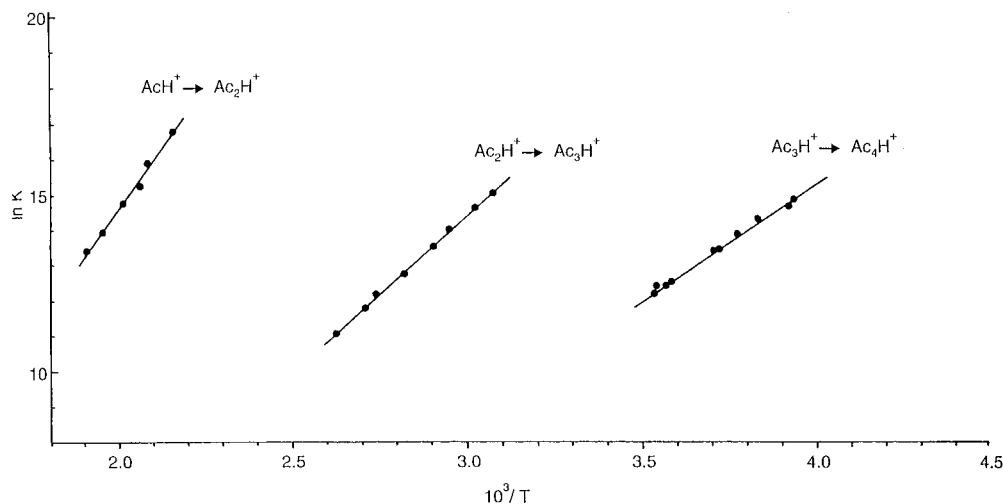


Figure 1. Van't Hoff plots for clustering reactions. Notation as in Scheme 1:  $T$  in degrees K,  $\ln K$  in units of  $\ln(\text{bar}^{-1})$ .

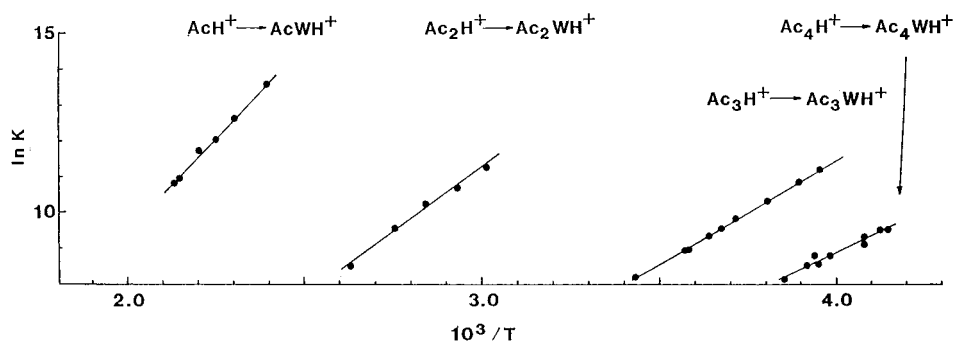


Figure 2. Van't Hoff plots for clustering equilibria. Notation as in Scheme 1:  $T$  in degrees K,  $\ln K$  in units of  $\ln(\text{bar}^{-1})$ .

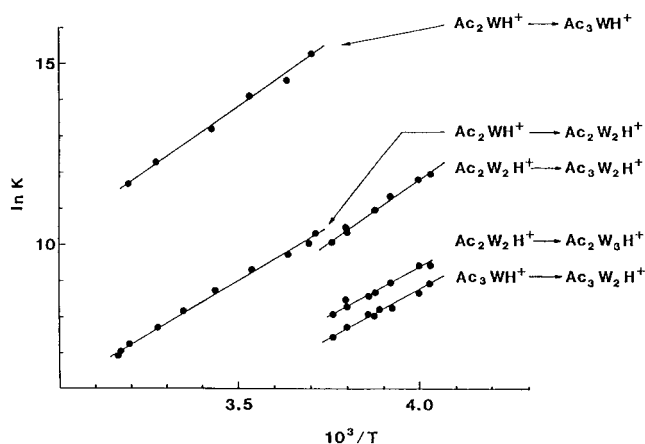
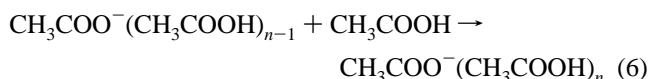
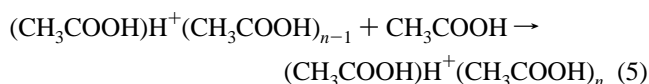


Figure 3. Van't Hoff plots for clustering equilibria. Notation as in Scheme 2:  $T$  in degrees K,  $\ln K$  in units of  $\ln(\text{bar}^{-1})$ .

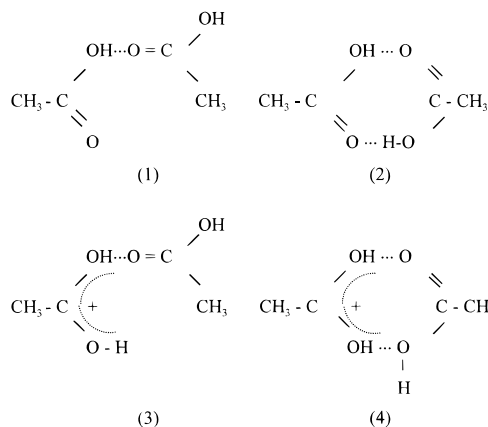
The variation of  $\Delta H_{n-1,n}^\circ$  with sequential clustering for equilibria 5 and 6 is shown in Figure 5.



First, it is interesting to compare the thermochemistry of dimer formation with other  $\text{OH}^+\cdots\text{O}$  type dimers. The value of  $\Delta H_D^\circ$

= 117.6 kJ/mol (28.1 kcal/mol) is somewhat smaller than for analogous dimers of water, methanol, dimethyl ether, and acetone, all of which are 126–138 kJ/mol (30–33 kcal/mol). It was suggested that forming the hydrogen bond perturbs the resonance stabilization of the monomer ion, resulting in decreased stability.<sup>21</sup> In contrast, in the anionic dimer,  $\Delta H_D^\circ = 122.6$  kJ/mol (29.3 kcal/mol) is similar to that of  $\text{CH}_3\text{O}^-(\text{CH}_3\text{OH})$ , 120.5 kJ/mol (28.8 kcal/mol), suggesting that resonance effects on the hydrogen bond are insignificant in this case.

As to geometries, the neutral and cationic dimers can exist in singly bonded or doubly bonded forms, ions 1–4. The doubly



bonded structures are expected to be more strongly bonded but also to have more negative entropies.

(21) Larson, J. W.; McMahon, T. B. *J. Am. Chem. Soc.* **1982**, *104*, 6255.

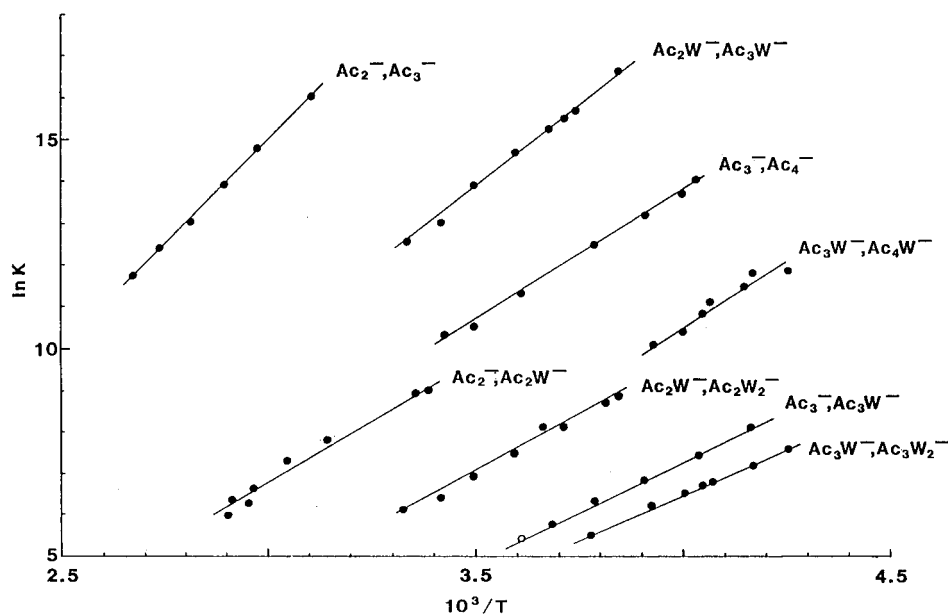


Figure 4. Van't Hoff plots for clustering equilibria. Notation as in Scheme 2:  $T$  in degrees K,  $\ln K$  in units of  $\ln(\text{bar}^{-1})$ .

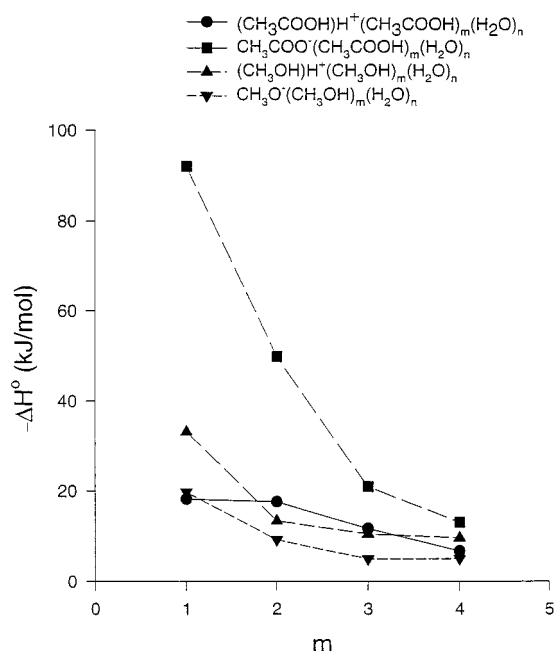


Figure 5. Enthalpy changes of  $\text{CH}_3\text{COOH}$  enrichment by substituting  $\text{CH}_3\text{COOH}$  for  $\text{H}_2\text{O}$  molecules in four-membered clusters, reactions 7 and 8, with  $m + n = 4$  and analogous reactions in methanol/water.

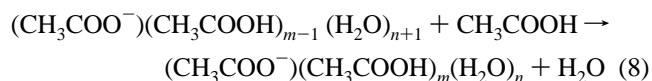
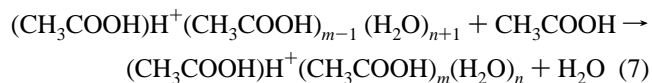
For the neutral  $(\text{AcH})_2$  dimer, isomer (1) with a single  $\text{OH} \cdots \text{O}$  bond should have a dissociation energy of about  $\Delta H^\circ_{\text{D}} = 21 \text{ kJ/mol}$  (5 kcal/mol) and  $\Delta S^\circ_{\text{D}} = 105 \text{ J/mol K}$  (25 cal mol<sup>-1</sup> K<sup>-1</sup>). The much larger literature values of  $\Delta H^\circ_{\text{D}} = 69.9 \text{ kJ/mol}$  (16.7 kcal/mol) and  $\Delta S^\circ_{\text{D}} = 176.2 \text{ J/mol K}$  (42.1 cal mol K) suggest that the doubly bonded isomer (2) was measured.<sup>13</sup> With the estimated thermochemistry for 1 and the experimental values for 2, the equilibrium ratio is  $K = [(2)]/[1)] > 1$  up to 684 K. This is consistent with the doubly bonded isomer (2) predominating in the range of 300–400 K where the neutral monomer–dimer equilibrium was measured in the literature.<sup>13</sup>

In contrast, for the ionic dimer  $(\text{AcH})_2\text{H}^+$  the measured bonding energy is comparable to other singly bonded  $\text{OH}^+ \cdots \text{O}$  dimers (with a small decrease due to resonance effects),

suggesting that isomer (3) dominates in the observed temperature range. From trends observed in polyfunctional ions, the bonding in the doubly bonded isomer (4) should be stronger by about 21 kJ/mol (5 kcal/mol), but the entropy of ion (4) should be more negative by about 42 J mol<sup>-1</sup> K<sup>-1</sup> (10 cal mol<sup>-1</sup> K<sup>-1</sup>) than in singly bonded complexes.<sup>2</sup> These values give  $K = [(4)]/[(3)] > 1$  up to 500 K, and the singly bonded isomer (3) is dominant at higher temperatures of 500–550 K, which is the experimental temperature range.

In summary, under our pressure and temperature conditions, both  $(\text{AcH})_2$ , as discussed in the Experimental Section, and  $(\text{AcH})_2\text{H}^+$  exist predominantly in the singly bonded form. However, at low temperatures, such as in clusters formed in cold supersonic beams, both the neutral and ionic dimers should exist in the double-bonded conformation.

**2. The Effects of Composition on the Stabilities of Hydrogen Bond Networks.** Schemes 1 and 2 show that replacing an  $\text{H}_2\text{O}$  molecule by a  $\text{CH}_3\text{COOH}$  molecule proceeding vertically up in the schemes, reactions 7 and 8, is always stabilizing.



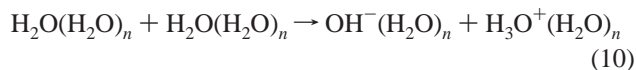
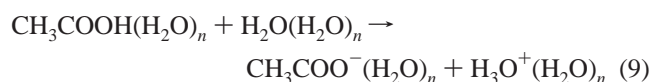
The increasing stabilization with  $\text{CH}_3\text{COOH}$  enrichment is characteristic of systems with unlimited hydrogen bond networks. The effect is largest in introducing the first  $\text{CH}_3\text{COOH}$  molecule into a neat water cluster, when the proton is transferred to the significantly more basic  $\text{CH}_3\text{COOH}$  molecule. The magnitude of the incremental stabilization decreases with increasing  $\text{CH}_3\text{COOH}$  content.

For each substitution step, the exothermicity of  $\text{CH}_3\text{COOH}$  enrichment is larger in the anionic than in the analogous cationic clusters. The trend is illustrated in Figure 5 for four-membered clusters. The figure also shows that the opposite applies in  $\text{CH}_3\text{OH}/\text{H}_2\text{O}$  clusters, where  $\text{CH}_3\text{OH}$  enrichment is more stabilizing in the cationic rather than in the anionic clusters. These trends

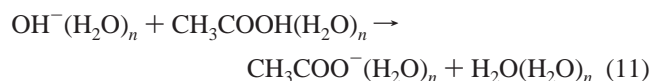
correlate with the relative acidity vs basicity of CH<sub>3</sub>COOH or CH<sub>3</sub>OH vs H<sub>2</sub>O. In CH<sub>3</sub>COOH/H<sub>2</sub>O, the  $\Delta H^\circ_{\text{acid}}$  difference is 175.7 kJ/mol (42.0 kcal/mol), larger than the PA difference of 91.2 kJ/mol (21.8 kcal/mol).<sup>22</sup> Since hydrogen bond strengths correlate with PAs and  $\Delta H^\circ_{\text{acid}}$  values,<sup>23–26</sup> replacement of H<sub>2</sub>O by CH<sub>3</sub>COOH molecules replaces a weaker acid with a much stronger neutral acid and substitutes weaker OH $\cdots$ O<sup>−</sup> bonds by stronger bonds. In the cationic CH<sub>3</sub>COOH/H<sub>2</sub>O clusters, the basicity difference between the components is smaller, and therefore, the effects of CH<sub>3</sub>COOH for H<sub>2</sub>O replacement are smaller. In comparison, the relative effects in the anionic and cationic clusters are reversed in CH<sub>3</sub>OH/H<sub>2</sub>O clusters. The  $\Delta H^\circ_{\text{acid}}$  difference between CH<sub>3</sub>OH and H<sub>2</sub>O is 38.5 kJ/mol (9.2 kcal/mol), smaller than the PA difference of 63.2 kJ/mol (15.1 kcal/mol),<sup>22</sup> and replacement of H<sub>2</sub>O molecules by CH<sub>3</sub>OH molecules strengthens the OH<sup>+</sup> $\cdots$ O bond network in the cationic clusters more than it strengthens the OH $\cdots$ O<sup>−</sup> bond network in the anionic clusters.

These results show that the hydrogen bond strengths in the assemblies reflect the relative acidities and basicities of the components. These relations apply through the addition of CH<sub>3</sub>-OH and CH<sub>3</sub>COOH molecules to the largest assemblies observed. Note that, in the large assemblies, complex structures may be present, including multiply hydrogen bonded ions and cyclic hydrogen bond systems as shown in the anion clusters below, or even containing neutral dimers, as indicated by dimer emission.<sup>27,28</sup> The results show that even when an added ligand is bonded by such complex interactions and when its addition affects a complex network, its acidity or basicity remains a determining factor of the bonding energy.

**3. The Effects of Partial Solvation on the Acidity and Basicity.** Clustering data was used in early studies by Kebarle to evaluate the effects of inner-shell ion solvation on acidities and basicities.<sup>1</sup> Reactions 9 and 10 represent acid dissociation (A<sup>−</sup>-H<sup>+</sup>) accompanied by the formation of an H<sub>3</sub>O<sup>+</sup> counterion, in the presence of *n* solvent molecules about each species, for two acids such as H<sub>2</sub>O and CH<sub>3</sub>COOH.



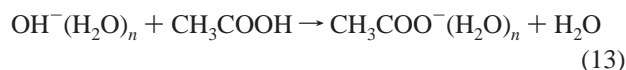
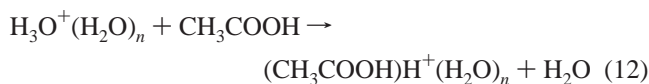
Subtracting eq 10 from eq 9 yields eq 11, which expresses the differential effects of solvation.



As eq 11 shows, the complete effects of *n*-fold hydration should include the hydration of the neutrals. However, the

difference between the energies of the neutral hydrogen bonds on the two sides of eq 11 should be small compared with the differences between the ion solvation energies. In fact, clustering energies of ions by four H<sub>2</sub>O molecules, without neutral clustering data, account well for relative bulk ion solvation energies.<sup>1–3</sup> Therefore, cluster thermochemistry can represent meaningfully the solvation effects on the relative enthalpies of ionization of CH<sub>3</sub>COOH vs H<sub>2</sub>O.

Subject to these considerations, the thermochemistry of reactions 12 and 13 reflects the effects of *n*-fold ion hydration on the relative acidity and basicity of CH<sub>3</sub>COOH vs H<sub>2</sub>O.



The results of eqs 12 and 13 are observed in Schemes 1 and 2, respectively, in the energy changes of the first step vertically up from the bottom row ions. The unsolvated CH<sub>3</sub>COOH molecule is a stronger base and acid than H<sub>2</sub>O (for *n* = 0,  $\Delta H^\circ_{12} = -91.1$  kJ/mol (−21.8 kcal/mol) and  $\Delta H^\circ_{13} = -175.7$  kJ/mol (−42.0 kcal/mol)). Four-fold hydration decreases both differences similarly, by −75.3 kJ/mol (−18.0 kcal/mol) for  $\Delta H^\circ_{12}$  and −88.7 kJ/mol (−21.2 kcal/mol) for  $\Delta H^\circ_{13}$ . This renders the protonation of CH<sub>3</sub>COOH in reaction 12 only slightly exothermic, by 15.8 kJ/mol (3.8 kcal/mol) in the largest clusters. However, in the anionic case, because of the large intrinsic acidity of CH<sub>3</sub>COOH, acid dissociation in reaction 13 still remains strongly exothermic, by 87.0 kJ/mol (20.8 kcal/mol).

The cluster data can be used to calculate the effects of solvation on acid dissociation using eq 9 by starting with CH<sub>3</sub>-COOH and H<sub>2</sub>O each solvated by *n* H<sub>2</sub>O molecules and forming the solvated ions. This process, as in solution, results in the strengthening of existing hydrogen bond assemblies due to the formation of the ions. The strength of the neutral hydrogen bonds can be estimated, noting that a single HOH $\cdots$ OH<sub>2</sub> bond is 21 kJ/mol (5 kcal/mol) while in solution an H<sub>2</sub>O molecule is bonded by a net of two hydrogen bonds by 44 kJ/mol (10.5 kcal/mol). We assume an increase by 4 kJ/mol (1 kcal/mol) per step, and we assume equal hydrogen bond strengths in CH<sub>3</sub>-COOH((H<sub>2</sub>O)<sub>*n*</sub>) and H<sub>2</sub>O(H<sub>2</sub>O)<sub>*n*</sub>. With these enthalpies in eq 9, the first four hydration steps decrease the acid dissociation enthalpy from 768 kJ/mol (184 kcal/mol) for the unsolvated acid by 158, 241, 306, and 332 kJ/mol (38, 58, 73, and 80 kcal/mol) through solvation by one to four H<sub>2</sub>O molecules. Correspondingly, the acid dissociation enthalpy decreases from 768 to 610, 527, 463, and 435 kJ/mol (from 184 to 146, 126, 111, and 104 kcal/mol.) After this step the value of  $\Delta H^\circ_9$  should not change significantly as the ion solvation enthalpies approach the neutral solvation enthalpies (see Tables 1 and 2) and the increments on the two sides of eq 9 cancel. However, the acid dissociation enthalpy of 435 kJ/mol (104 kcal/mol) of the four-fold hydrated cluster remains much more endothermic than the solution value of −0.2 kJ/mol (−0.06 kcal/mol). These observations are in accordance with the well-known trend that clustering reproduces the relative ion hydration energies but approaches the absolute ion hydration energies very slowly.<sup>2,3</sup>

When methanol and acetic acid are compared, proton transfer from CH<sub>3</sub>OH<sub>2</sub><sup>+</sup> to CH<sub>3</sub>COOH is exothermic by 28.0 kJ/mol (6.7 kcal/mol), but as calculated from the present and literature data,<sup>10</sup> the sign reverses and the process becomes endothermic by 17.6 kJ/mol (4.2 kcal/mol) in the 4-fold hydrated species.

(22) Lias, S. G.; Bartmess, J. E.; Liebman, J. F.; Holmes, J. L.; Levin, R. D.; Mallard, W. G. Ion Energetics Data. In *NIST Standard Reference Database Number 69*; Mallard, W. G., Linstrom, P. J., Eds.; National Institute of Standards and Technology: Gaithersburg, MD 20899, August 1997 (<http://webbook.nist.gov>).

(23) Yamdagni, R.; Kebarle, P. *J. Am. Chem. Soc.* **1973**, *95*, 3504.

(24) Larson, W. J.; McMahon, T. B. *J. Am. Chem. Soc.* **1984**, *106*, 517.

(25) Meot-Ner (Mautner), M. In *Molecular Structure and Energetics*; Greenberg, A., Liebman, J. F., Eds.; VCH Publishers: Deerfield Beach, FL; 1987, Vol. 4, p 71.

(26) Meot-Ner (Mautner), M. *J. Am. Chem. Soc.* **1984**, *106*, 1265; *J. Am. Chem. Soc.* **1992**, *114*, 3312.

(27) Lifshitz, C.; Feng, W. Y. *Int. J. Mass Spectrom. Ion Processes* **1995**, *146*, 223.

(28) Feng, W. Y.; Lifshitz, C. *J. Mass Spectrom.* **1995**, *30*, 1179.

**Table 1.** Ab Initio Energetics of Complexation To Form  $\text{CH}_3\text{COO}^-(\text{CH}_3\text{COOH})_m(\text{H}_2\text{O})_n^a$ 

	$\text{Ac}^-(\text{W})$ (A)	$\text{Ac}^-(\text{W})$ (B)	$\text{Ac}^-(\text{W})_2$ (A)	$\text{Ac}^-(\text{W})_2$ (B)	$\text{Ac}^-(\text{AcH})$	$\text{Ac}^-(\text{AcH})(\text{W})$
$\Delta E_{\text{elec}}$ (SCF/4-31G)	-86.2	-102.9	-159.4	-187.0	-141.0	-213.8
$\Delta H_{\text{calcd}}$ (SCF/4-31G)	-78.2	-93.3	-143.1	-168.2	-136.0	-198.7
$\Delta E_{\text{elec}}$ (MP2/6-31G*)	-72.8	-89.1	-134.3	-158.2	-121.3	-185.8
$\Delta H_{\text{calcd}}$ (MP2/6-31G*)	-64.4	-79.1	-118.0	-139.3	-115.9	-170.7
$\Delta H_{\text{exp}}$	-66.5 <sup>b</sup>	-66.5 <sup>b</sup>	-120.5 <sup>b</sup>	-120.5 <sup>b</sup>	-122.6 <sup>b</sup>	-174.1 <sup>b</sup>

<sup>a</sup> Complexation energies defined relative to isolated, optimized constituents. All quantities in kilojoules per mole. For structures, see Figures 7–12 and the Supporting Information. <sup>b</sup> Isomeric structure of the measured clusters is not known and may involve mixtures of isomers.

**Table 2.** Ab Initio Energetics of Complexation To Form  $\text{CH}_3\text{COO}^-(\text{CH}_3\text{COOH})(\text{H}_2\text{O})_2^a$ 

isomer	A	B	C	D	E	F	G
$\Delta E_{\text{elec}}$ (SCF/4-31G)	-266.9	-272.8	-282.0	-291.2	-294.5	-285.4	-291.6
$\Delta H_{\text{calcd}}$ (SCF/4-31G)	-243.9	-249.8	-259.4	-265.3	-268.6	-265.3	-270.3
$\Delta E_{\text{elec}}$ (MP2/6-31+G*)	-223.8	-226.8	-241.0	-245.2	-246.9	-236.8	-252.3
$\Delta H_{\text{calcd}}$ (MP2/6-31+G*)	-200.8	-203.8	-218.4	-219.2	-220.9	-216.7	-231.0

<sup>a</sup> Complexation energies defined relative to isolated, optimized constituents. All quantities in kilojoules per mole. Compare with experimental complexation energy of -219.7 kJ/mol. For structures, see Figure 12 and the Supporting Information.

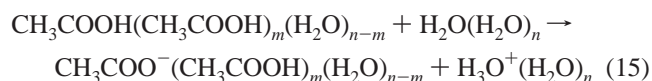
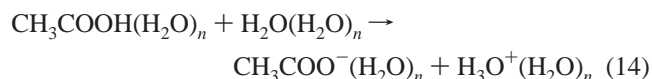
This suggests that methanol should be a stronger base than acetic acid in aqueous solution because of solvation effects. The relative acidities are affected even more strongly, where proton transfer from  $\text{CH}_3\text{COOH}$  to  $\text{CH}_3\text{O}^-$  is exothermic by 137.2 kJ/mol (32.8 kcal/mol) for the unsolvated species, decreasing to 78.2 kJ/mol (18.7 kcal/mol) in the 4-fold hydrated species. Nevertheless,  $\text{CH}_3\text{COOH}$  remains the stronger acid because of the large intrinsic acidity difference.

The clustering data therefore show that specific hydrogen bonding of the ions to the first four  $\text{H}_2\text{O}$  molecules halves the intrinsic  $\Delta H_{\text{acid}}^\circ$  difference between methanol and acetic acid. Inner-shell ion solvation has as much effect on the solution acidities as the intrinsic molecular acidities themselves.

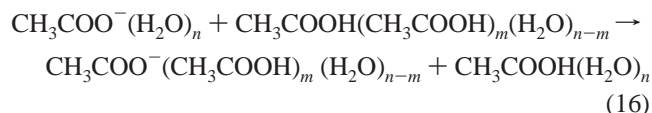
#### 4. The Effects of Aggregation on the Acidity and Basicity.

In concentrated solutions, in polyelectrolytes, and in biological systems, carboxylate groups are often close enough to form hydrogen bonds. After protonation or deprotonation, the neutral hydrogen bonds are converted into  $(\text{RCOOH})\text{H}^+\cdots\text{RCOOH}$  or  $\text{RCOO}^-\cdots\text{HOOCR}$  bonds. The effects are similar but stronger than the solvation effects discussed in the previous section.

Acid dissociation in dilute solution with formation of the  $\text{H}_3\text{O}^+$  counterion is modeled by eq 14, where each ion is solvated by  $n$   $\text{H}_2\text{O}$  molecules. With aggregation where  $m$   $\text{CH}_3\text{COOH}$  molecules displace  $m$   $\text{H}_2\text{O}$  molecules, the reaction is modeled by eq 15.



The effect of aggregation with solvent displacement on the acidity is obtained by subtracting eq 14 from eq 15, resulting in eq 16.



Similar to the preceding section, for models of linear  $\text{OH}\cdots\text{O}$  bonded chains (excluding strong multiply bonded  $(\text{CH}_3\text{COOH})_n$  aggregates), the solvation of the neutrals approximately

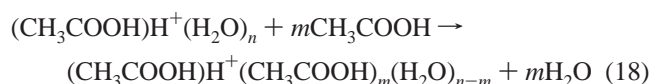
cancels on both sides of eq 16. Therefore the clustered neutrals may be substituted by the gas-phase neutrals in reaction 17.



The thermochemistry is obtained by proceeding upward from the second row in each column in Scheme 2.

The formation of the dimer  $\text{CH}_3\text{COO}^-(\text{CH}_3\text{COOH})(\text{H}_2\text{O})_n$  with the displacement of one  $\text{H}_2\text{O}$  molecule is given by  $\Delta H_{17}^\circ$  for  $m = 1$ , possibly in the presence of  $n$  additional solvent molecules. In the absence of additional solvation, with  $n = 0$ , dimer formation with solvent displacement stabilizes the anion by an additional 56.0 kJ/mol (13.4 kcal/mol), and therefore the acid dissociation enthalpy decreases by this amount. In the presence of one or two additional  $\text{H}_2\text{O}$  molecules the effect of dimer formation is only slightly smaller, 53.6 (12.8) and 49.8 (11.9) kJ/mol (kcal/mol), respectively.

Similar considerations apply also to the effects of aggregation on the thermochemistry of protonation.



The thermochemistry is obtained by proceeding upward from the second row in each column in Scheme 1. Protonation accompanied by dimer formation with solvent displacement results in  $(\text{CH}_3\text{COOH})\text{H}^+(\text{CH}_3\text{COOH})$ , which stabilizes the ion by an additional 32.2 kJ/mol (7.7 kcal/mol) compared with solvation by one  $\text{H}_2\text{O}$  molecule, and therefore makes the enthalpy of protonation more negative by this amount. The effect of dimer formation with solvent replacement is somewhat smaller, 20.5 (4.9), 17.1 (4.1), and 14.6 (3.5) kJ/mol (kcal/mol) in the presence of one, two, and three further  $\text{H}_2\text{O}$  molecules, respectively.

The results show that in both acid dissociation and protonation, the effects of the first aggregation step to form the dimer with the displacement of an  $\text{H}_2\text{O}$  molecule are affected little by the presence of further water molecules. Extrapolation to the condensed phase would suggest that dimer formation with the displacement of an  $\text{H}_2\text{O}$  molecule can make acid dissociation more exothermic by about 50 kJ/mol (12 kcal/mol) and

protonation more exothermic by about 15 kJ/mol (3.5 kcal/mol) than forming only the monomer ions.

Higher aggregation enhances these effects. For example, the formation of the  $\text{CH}_3\text{COO}^-(\text{CH}_3\text{COOH})_3$  aggregate makes  $\Delta H^\circ_{17}$  more negative by 83.7 kJ/mol (20.0 kcal/mol), compared with the formation of  $\text{CH}_3\text{COO}^-(\text{H}_2\text{O})_3$ . In protonation, the formation of  $(\text{CH}_3\text{COOH})\text{H}^+(\text{CH}_3\text{COOH})_3$  aggregate makes  $\Delta H^\circ_{18}$  more negative by 35.5 kJ/mol (8.5 kcal/mol), compared with the protonation of the monomeric carboxylic function that forms  $(\text{CH}_3\text{COOH})\text{H}^+(\text{H}_2\text{O})_3$ .

In addition to the effect on the anion product of acid dissociation, aggregation in concentrated solutions can also enhance acid dissociation by stabilizing the released proton. In dilute solution, the proton may remain in aqueous solution as the high intrinsic basicity of  $\text{CH}_3\text{COOH}$  vs  $\text{H}_2\text{O}$  is nearly canceled even by partial solvation, as discussed above. For example, proton transfer from  $\text{H}_3\text{O}^+$  to  $\text{CH}_3\text{COOH}$  is exothermic by 91.1 kJ/mol (21.8 kcal/mol) in the unsolvated species but only slightly exothermic, by 18.7 kJ/mol (4.5 kcal/mol), in the 4-fold solvated clusters  $(\text{H}_2\text{O})_4$  vs  $\text{CH}_3\text{COOH}(\text{H}_2\text{O})_3$ . This trend suggests that proton transfer from  $\text{H}_3\text{O}^+$  to form  $(\text{CH}_3\text{COOH})\text{H}^+$  may be endothermic. However, Scheme 1 shows that the proton is solvated more strongly in  $(\text{CH}_3\text{COOH})_4\text{H}^+$  than in  $(\text{H}_2\text{O})_4\text{H}^+$  by 54.2 kJ/mol (13.0 kcal/mol). These trends suggest that in dilute aqueous solution of carboxylic acids the proton may be located preferentially on a hydronium ion, but in concentrated solutions, the proton may be more stabilized in a carboxylic acid aggregate. This can make acid dissociation more exothermic in concentrated solutions.

**5. Self-Assembly of Carboxylic Acids Compared with Other Functional Molecules.** As discussed above, ion-neutral aggregation in solution constitutes the replacement of solvent molecules by solute molecules in the inner shell. The thermochemistry is represented by the substitution reactions 7 and 8, proceeding vertically up in Schemes 1 and 2, and similarly for other mixed clusters. Figure 6 shows that aggregation about ions with solvent displacement is much more favorable for carboxylic acids than for other functionalized molecules. This results from a combination of strong bonding of the carboxylate ion to carboxylic acid molecules and weak bonding to solvent molecules. For example, the bond strength in  $\text{CH}_3\text{COO}^-(\text{CH}_3\text{COOH})$  is 122.6 kJ/mol (29.3 kcal/mol), compared with the weak bond strength in  $\text{CH}_3\text{COO}^-(\text{H}_2\text{O})$ , which is 66.5 kJ/mol (15.9 kcal/mol). The weak bonding to solvent results from the large  $\Delta H^\circ_{\text{acid}}$  difference between  $\text{CH}_3\text{COOH}$  and  $\text{H}_2\text{O}$  (175.7 kJ/mol (42.0 kcal/mol)),<sup>22</sup> according to the correlation between the relative acidities of the components and hydrogen bond strengths.<sup>23–25</sup>

Ionic aggregation with solvent displacement is less favorable for other functional groups because of weaker hydrogen bonds to the parent molecules compared with carboxylic acids, or because stronger bonds to the solvent disfavor displacement. For example, in protonated amines, the formation of the ion-neutral dimer is less favorable because the strength of the  $\text{NH}^+\cdots\text{N}$  bond, 100 kJ/mol (24 kcal/mol), is weaker than the 125 kJ/mol (30 kcal/mol) strength of  $\text{OH}\cdots\text{O}^-$  bonds.<sup>23–26</sup> In protonated alcohols, ketones, and acids and in deprotonated alcohols the bonding energy of the dimer is similar to that in  $\text{CH}_3\text{COO}^-(\text{CH}_3\text{COOH})$ , but these ions are bonded more strongly to the solvent  $\text{H}_2\text{O}$  molecules because of the smaller  $\text{PA}$  or  $\Delta H^\circ_{\text{acid}}$  differences between these compounds and water,<sup>23–26</sup> making solvent displacement less favorable.

These trends can be extended to larger clusters and possibly to solution, because the relative energies of aggregation should not be affected significantly in larger clusters when the

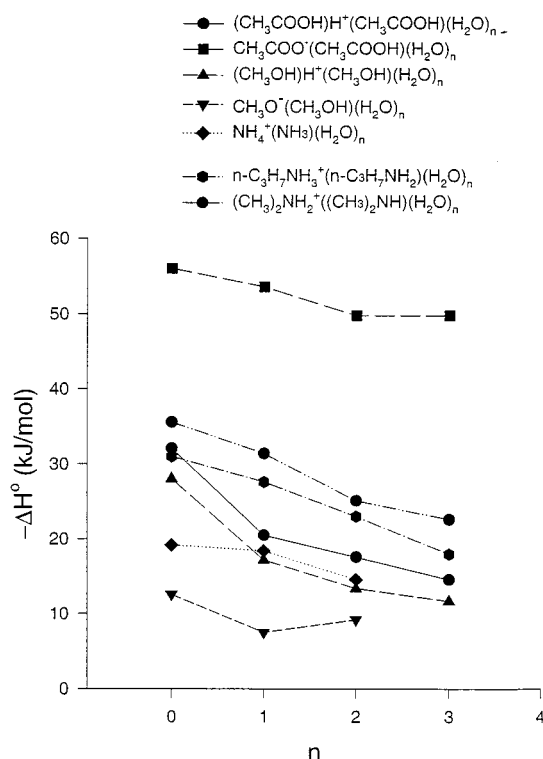


**Figure 6.** Enthalpy sequences for dimerization with solvent displacement as a function of increasing solvation  $n$  as shown. Here  $n$  denotes the number of solvent molecules remaining after one is replaced by the organic ligand molecule. Data for ammonia/water from ref 9, for methanol/water from ref 10, and for  $n$ -propylamine and dimethylamine from Meot-Ner (Mautner), 1997, unpublished results.

enthalpies of addition of  $\text{H}_2\text{O}$  molecules on both sides of eqs 7 and 8 approach the 42 kJ/mol (10.5 kcal/mol) condensation energy limit. This would predict that ionic aggregates of carboxylic acids in aqueous solution are more stable than ionic aggregates of other functionalized molecules, favoring the self-assembly of carboxylic acids to form micelles and membranes.<sup>29</sup>

### Computational Results

We used ab initio calculations to examine the complexes of the acetate ion with up to three neutral molecules. The primary purpose of the computations, at the levels affordable for these large systems, is to identify possible stable multiply hydrogen bonded structures. Results using the 4-31G basis set are reported in Figures 7–12 and in the Supporting Information. Bonding energies for these geometries calculated on a higher level using the basis set MP2/6-31+G\* are reported in Tables 1 and 2. The enthalpies computed at this level are substantially closer to the experimental results than with the 4-31 G set, although the structures optimized with SCF/4-31G are not necessarily the minima on the MP2/6-31+G8 surface. At any rate, since all the complexes involve one ionic species, the computational overestimate of the ionic interactions should be comparable in the various isomeric clusters with the same composition and, in fact, the relative energies are similar on the lower or higher level. In the comparison with experiment, note also that the isomers observed experimentally may not be the lowest-energy structures, as entropy effects may render higher-energy isomers dominant.

The geometries and charge densities computed for the separated monomers are shown in Figure 7, for comparison with

(29) Hargreaves, W. R.; Deamer, D. W. *Biochemistry* **1978**, *17*, 3759.



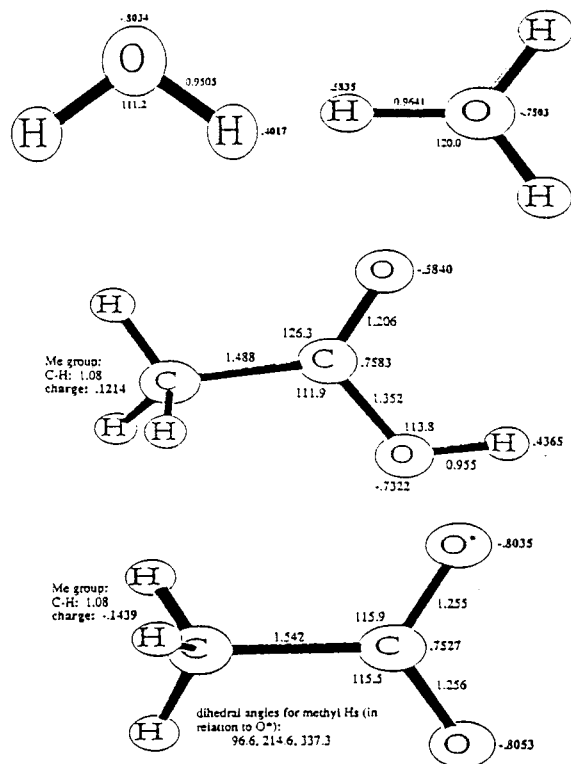


Figure 7. Computed geometries and Mulliken atomic charges for cluster components.

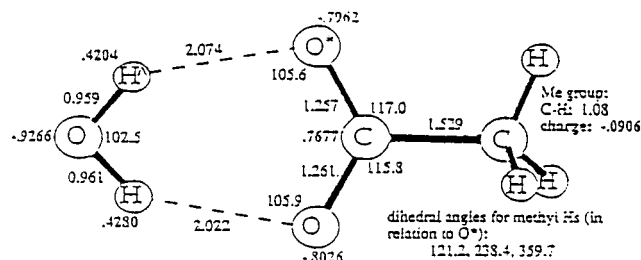


Figure 8. Computed geometries and Mulliken atomic charges for  $\text{CH}_3\text{COO}^-(\text{H}_2\text{O})$ , isomer B.

the geometries and charge densities altered by hydrogen bonding in the complexes.

In the first complex,  $\text{CH}_3\text{COO}^-(\text{H}_2\text{O})$ , in Figure 8, there are two minima. The first, isomer A in Table 1, involves a single hydrogen bond with the  $\text{H}_2\text{O}$  and  $\text{CH}_3\text{COOH}$  rotated by  $180^\circ$  about the hydrogen bond. The second structure, isomer B, has a nearly  $C_{2v}$  symmetry in that each hydrogen atom the  $\text{H}_2\text{O}$  molecule forms a hydrogen bond to an O atom of the acetate. The extra hydrogen bond makes isomer B more stable by 15.1 kJ/mol (3.6 kcal/mol) than isomer A on the SCF/4-31 G level, but the constraint decreases the computed entropy on the 4-31G level by 14.6 J mol $^{-1}$  K $^{-1}$  (3.5 cal mol $^{-1}$  K $^{-1}$ ). The added stability of 14.7 kJ/mol (3.6 kcal/mol) is confirmed by the MP2/6-31+G\* calculations.

In  $\text{CH}_3\text{COO}^-(\text{H}_2\text{O})_2$  in Figure 9, two minima are again identified. In both isomers, one  $\text{H}_2\text{O}$  molecule bonds to each of the acetate O atoms. In the less stable isomer A in Table 1 the two  $\text{H}_2\text{O}$  molecules are pointed away from each other and do not interact. The more stable energy isomer B contains a hydrogen bond between the two  $\text{H}_2\text{O}$  molecules. The extra bond in the system makes this isomer significantly more stable, by 25.1 kJ/mol (6.0 kcal/mol) or by 21.3 kJ/mol (5.1 kcal/mol) with MP2/6-31+G\*, but the calculated entropy difference on the 4-31G level is more unfavorable for this isomer by 69.9 J

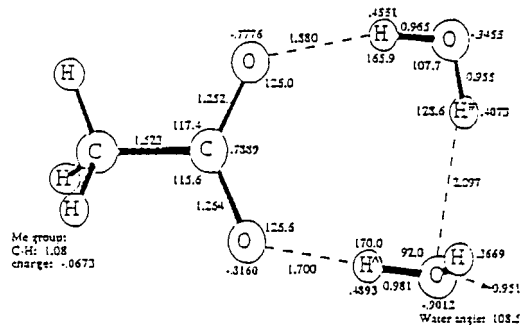


Figure 9. Computed geometries and Mulliken atomic charges for  $\text{CH}_3\text{COO}^-(\text{H}_2\text{O})_2$ , isomer B.

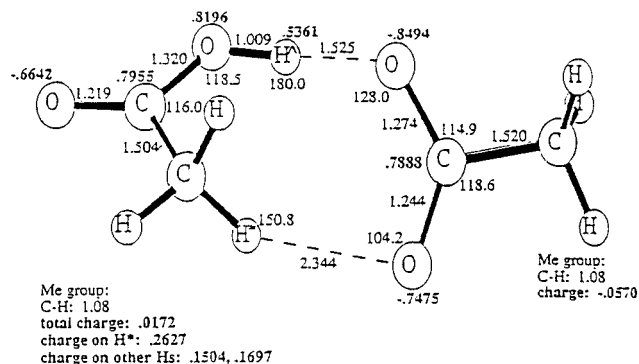


Figure 10. Computed geometries for and Mulliken charges for  $\text{CH}_3\text{COO}^-(\text{CH}_3\text{COOH})$ .

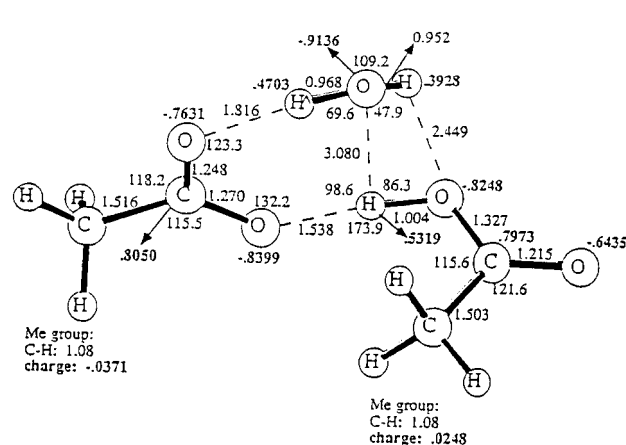


Figure 11. Computed geometries and Mulliken charges for  $\text{CH}_3\text{COO}^-(\text{CH}_3\text{COOH})(\text{H}_2\text{O})$ .

mol $^{-1}$  K $^{-1}$  (16.7 cal mol $^{-1}$  K $^{-1}$ ). In terms of free energies at 298 K, the stabilities of the isomers are comparable.

For the dimer  $\text{CH}_3\text{COO}^-(\text{CH}_3\text{COOH})$ , only the minimum shown in Figure 10 was found. The computed binding enthalpy of this complex is 136.0 kJ/mol (32.5 kcal/mol) or 115.9 kJ/mol (27.7 kcal/mol) and, with MP2/6-31+G\*, is close to the experimental value. In addition to the  $\text{OH}\cdots\text{O}^-$  bond, there is another weaker interaction between the methyl group of the acetate and the second oxygen of the acetate ion. This  $\text{CH}\cdots\text{O}^-$  bond is likely weak, as the  $\text{H}\cdots\text{O}$  distance is 0.2344 nm. We note that a higher-level calculation for the analogous  $\text{HCOO}^-(\text{HCOOH})$  dimer also found a doubly bonded structure with a  $\text{CH}\cdots\text{O}^-$  contribution.<sup>30</sup>

In  $\text{CH}_3\text{COO}^-(\text{CH}_3\text{COOH})(\text{H}_2\text{O})$  in Figure 11, the most stable minimum contains a network of four hydrogen bonds. Each component is hydrogen-bonded directly to each of the other

(30) Basch, H.; Stevens, W. J. *J. Am. Chem. Soc.* **1991**, *113*, 95.

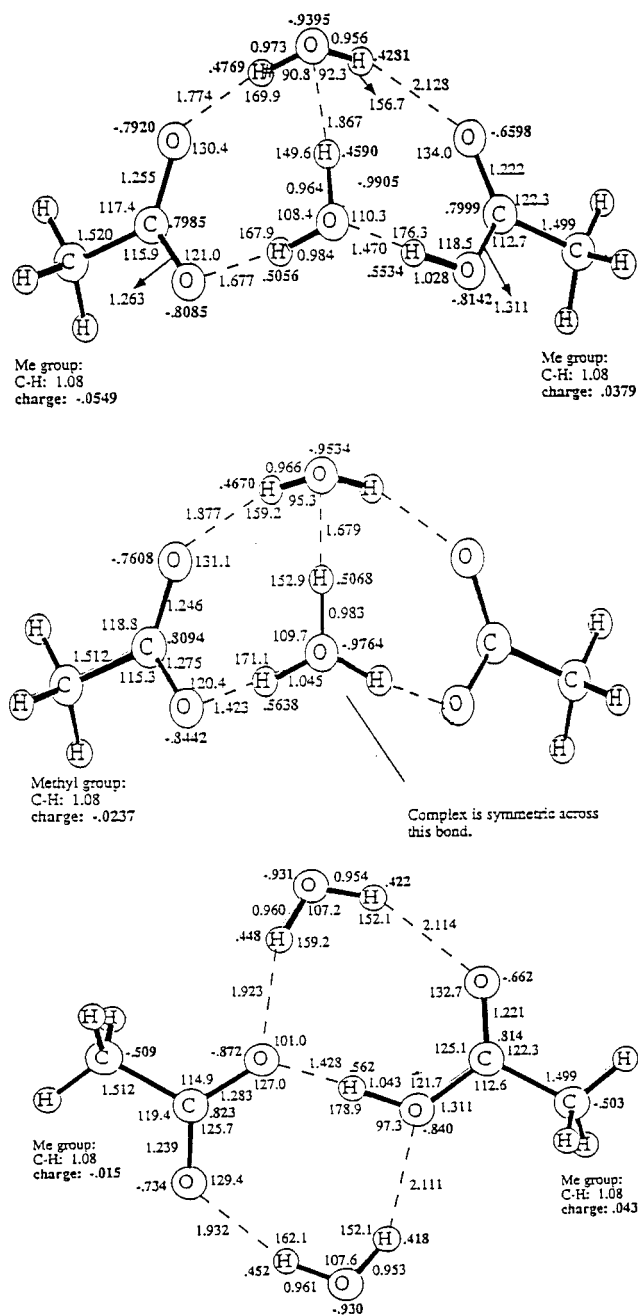


**Figure 12.** Computed geometries and Mulliken atomic charges, for  $\text{CH}_3\text{COO}^-(\text{CH}_3\text{COOH})(\text{H}_2\text{O})_2$ , isomer E (top), isomer F (middle), isomer G (bottom).

components, with two hydrogen bonds between the two ligands. Again the MP2/6-31+G\* binding enthalpy of 170.7 kJ/mol (40.8 kcal/mol) is rather close to the experimental binding enthalpy.

The largest computed complex is  $\text{CH}_3\text{COO}^-(\text{CH}_3\text{COOH})(\text{H}_2\text{O})_2$ . Seven minima were located as shown in Table 2. The energies and enthalpies of five of the seven isomers are comparable within 15.6 kJ/mol (3.8 kcal/mol) on both levels of calculation. Three structures corresponding to local minima and a proton-transfer transition state are shown in Figure 12.

We note that only in three of the seven minima is there a direct bond between acetate and acetic acid. Even in these isomers, further bridging between the acetate and acetic acid occurs by water molecules. In the other energy minima, the structure is bridged entirely by one or two water molecules, without direct bonding between the acetate and acetic acid components. In fact, the most stable structure is such a bridged structure.

The least stable isomer, A in Table 2, involves no direct  $\text{OH}\cdots\text{O}^-$  bond between the acetate and acetic acid, only a bond through the methyl group of the neutral and a bridging water molecule. In the next least stable structure, isomer B, only one water molecule is bridging by two water hydrogen bonds, and the other water molecule is bonded on the periphery. These high-energy structures are not shown in the figure.

Proceeding to lower-energy structures, isomer C is the only local minimum that contains a direct bond between the acetate ion and acetic acid plus one bridging water molecule, while the other water molecule provides a supporting peripheral bridge with a bond to the first  $\text{H}_2\text{O}$  molecule as a hydrogen receptor and to the acetate ion as a hydrogen donor. However, the next more stable isomer, D, has no direct bond and is bridged by only one water molecule, with the other water molecule providing a supporting peripheral bridge. The next lower-energy structures E and F are bridged by two water molecules. Finally, in the most stable isomer, G, there is a direct acetate/acetic acid bond and also two bridging water molecules.

While the binding energies and enthalpies computed at the more reliable MP2/6-31+G\* level are somewhat smaller than SCF/4-31G, the results are quite consistent at either level. At both levels, the A and B geometries are less stable than the others. The remaining configurations, C–G, are close in enthalpy, within 10.9 kJ/mol (2.6 kcal/mol) with SCF/4-31G or within 14.3 kJ/mol (3.4 kcal/mol) on the MP2/6-31+G\* level.

Probably the most interesting species is F, which is formed from E by proton transfer from the neutral acetic acid molecule to a bridging water molecule. This species can be described as a pair of acetate anions bridged by an  $\text{H}_3\text{O}^+$  ion and one  $\text{H}_2\text{O}$  molecule. This charge-separated species is not a local minimum, but rather a transition state on a nearly flat surface, which is less stable only by 3.4 kJ/mol (0.8 kcal/mol) or 4.2 kJ/mol (1.0 kcal/mol) with MP2/6-31+G\* than the parent structure E. Although a local transition state, it has a lower energy than some of the local minima that correspond to non-charge-separated isomers. The ease of proton transfer from the neutral carboxylic acid group in isomer E to the water O atom to form this isomer may be due in part to the already large negative charge on the water O atom in isomer E, due to the bond to the ionized carboxylate group.

In the proton transfer to form the species F, the overall charge of  $-0.026$  on the bridging water molecule changes to  $+0.658$  in the  $\text{H}_3\text{O}^+$  ion. The charge on the acetate O atoms participating in the bridge becomes more negative, and each carboxylate group carries a charge of  $-0.796$ . The structure assumes a symmetric geometry that is a suitable intermediate for proton transfer between the carboxylic groups.

Note that in isomer F the proton is located on an  $\text{H}_2\text{O}$  molecule adjacent to  $\text{CH}_3\text{COO}^-$  groups, although the proton affinity of  $\text{H}_2\text{O}$  is lower by as much as 768 kJ/mol (184 kcal/mol) than the carboxylate ions. Similar cases were observed where an  $\text{H}_3\text{O}^+$  ion was between two  $\text{CH}_3\text{CN}$ , ether or ketone groups that have proton affinities higher by up to 170 kJ/mol (40 kcal/mol) than the central  $\text{H}_2\text{O}$  molecule.<sup>7,31–33</sup> Evidence was found also for a similar structure involving  $\text{H}_3\text{O}^+$  and two  $(\text{CH}_3)_3\text{N}$  molecules,<sup>34</sup> where the PA difference is 270 kJ/mol (65 kcal/mol).<sup>22</sup> These structures can be seen as a compromise geometry where the strong bases attract the proton in opposite

(31) Meot-Ner (Mautner), M. *J. Am. Chem. Soc.* **1994**, *116*, 7848.

(32) Sharma, R. B.; Kebarle, P. *J. Am. Chem. Soc.* **1984**, *106*, 6193.

(33) Wei, S.; Tzeng, W. B.; Castleman, A. W. *J. Phys. Chem.* **1991**, *95*, 585. Wei, S.; Tzeng, W. B.; Castleman, A. W. *Z. Phys. D.* **1991**, *20*, 47.

(34) Meot-Ner (Mautner), M.; Scheiner, S.; Yu, W. O. *J. Am. Chem. Soc.* **1998**, *120*, 6980.

directions, and it becomes located in a balanced position on the less basic molecule in the center. Structure F represents an extreme example, where the proton is located on  $\text{H}_3\text{O}^+$  bridging between two anions whose proton affinities are higher by 768 kJ/mol (184 kcal/mol) when they are separated gas-phase species.

The general observation from the computed results is that there is little difference in the energetics whether the carboxylic acid and carboxylate are in direct contact or are bridged by water molecules or whether the ligand system constitutes only neutrals or a charge-separated ion pair.

## Conclusions

The effects of partial solvation on the acidity, basicity, and self-assembly of acetic acid were examined by measurements of cluster thermochemistry. Acetic acid is a strong intrinsic acid and base and its ionized forms bond strongly to carboxylic groups, while the correlations with hydrogen bond strengths lead to relatively weak bonding to solvent molecules. These relations determine the thermochemistry of mixed ionized acetic acid/water aggregates. The resulting effects in the 4-fold hydrated clusters nearly eliminate the exothermicity of proton transfer from  $\text{H}_2\text{O}$  to  $\text{CH}_3\text{COOH}$  molecules and reverse the intrinsic molecular proton affinity order between  $\text{CH}_3\text{OH}$  and  $\text{CH}_3\text{-COOH}$ . The relative acidities are affected similarly, but because of its strong intrinsic acidity, acetic acid remains a stronger acid than water and methanol in the 4-fold hydrated clusters, as well as in aqueous solution.

The cluster models show that aggregation in concentrated solutions can significantly enhance acid dissociation by stabilizing the carboxylate anion by  $\text{CH}_3\text{COO}^- \cdots \text{HOOCCH}_3$  bonds and the released proton in  $(\text{CH}_3\text{COOH})_n(\text{H}_2\text{O})_m\text{H}^+$  assemblies.

The clustering results explain why self-assembly and membrane formation is particularly favorable in ionized carboxylic acids, compared with other types of functionalized molecules.<sup>32</sup> The effect results from the strengths of hydrogen bonds between various components due to the correlations with the relative acidities and basicities. First, the bonding strength in many  $\text{OH}^+ \cdots \text{O}$  and  $\text{O}^- \cdots \text{HO}$  dimers is about 125 kJ/mol (30 kcal/mol). This is stronger than in  $\text{NH}^+ \cdots \text{N}$  bonds, 100 kJ/mol (24 kcal/mol), and therefore oxygen functional groups will tend more to ion-neutral association than amines. However, ionized oxygen groups such as  $(\text{ROH})\text{H}^+$  and  $\text{RO}^-$  ions bond relatively strongly to  $\text{H}_2\text{O}$  molecules because of the relatively small PA and  $\Delta H^\circ_{\text{acid}}$  difference between alcohols and  $\text{H}_2\text{O}$ , making solvent displacement unfavorable. Conversely, because of the strong intrinsic acidity of the carboxylic group, correlations with the acidities result in weak bonding to solvent molecules. The trends in Figure 6 show that the combination of strong  $\text{RCOO}^- \cdots \text{HOOCR}$  bonds and weak  $\text{RCOO}^- \cdots \text{H}_2\text{O}$  bonds to solvent molecules makes aggregation with solvent displacement particularly favorable for carboxylate-carboxylic acid systems.

Three interesting computational results on the  $\text{CH}_3\text{COO}^- (\text{CH}_3\text{COOH})(\text{H}_2\text{O})_2$  clusters are the following: (1) a variety of geometries are comparable in stability; (2) directly bonded and solvent-bridged isomers have comparable stabilities; and (3) the

bridging  $\text{H}_2\text{O}$  molecule allows a low-energy pathway for proton transfer through an  $\text{H}_3\text{O}^+$  bridged intermediate.

These results have potential biological implications. Acid dissociation of carboxylic acid groups in membranes and proteins can be facilitated by the proximity of other carboxylic groups by forming strong  $\text{RCOO}^- \cdots \text{HOOCR}$  bonds. This need not require a strict positioning of the carboxylic groups, as several geometries can allow strong ion-neutral hydrogen bonds and bridging water molecules can mediate these stabilizing interactions between separated carboxylic groups.

We noted the small energy difference between the charge-separated structure F and the other isomers in Table 2. This charge-separated isomer arises by proton transfer from the neutral carboxylic group in isomer E. Subsequent proton transfer to the other carboxylate ion amounts to overall proton transfer between the two carboxylic groups through the bridging water molecule. This is similar to proton transfer between ether or carbonyl groups through water bridges that model proton transport in membranes.<sup>34</sup> In both cases, the proton moves by bond rearrangement in a hopping mechanism rather than physical diffusion, similar to proton transport in water. Through this mechanism, solvent bridges can provide low-energy pathways for proton transfer.

In general conclusion, ionic hydrogen bond strengths correlate with the intrinsic acidities and basicities of the components.<sup>1-6</sup> These relations have broad significance. They affect ion solvation, acidities and basicities in solution, aggregation, self-assembly, and the energetics of membranes and enzymes. The correlations between molecular acidities and basicities and ionic hydrogen bond strengths, first observed in dimers,<sup>1-6</sup> therefore also have fundamental effects in complex ionic hydrogen bonded assemblies.

**Acknowledgment.** We thank the late Dr. L. Wayne Sieck for the use of the NIST mass spectrometer and for helpful discussions, and we wish to commemorate his work with this article. We also thank the NIH for a grant for partial support of this work.

**Supporting Information Available:** Geometries and Mulliken charge distributions of high-energy isomers calculated on the 4-31G level: isomer A (Table 3) of  $\text{CH}_3\text{COO}^- (\text{H}_2\text{O})$  with single hydrogen bond; isomer A (Table 3) of  $\text{CH}_3\text{COO}^- (\text{H}_2\text{O})_2$  with two noninteracting  $\text{H}_2\text{O}$  molecules; isomer A (Table 4) of  $\text{CH}_3\text{COO}^- (\text{CH}_3\text{COOH})(\text{H}_2\text{O})_2$  with a  $-\text{CH}_3 \cdots \text{O}^- \text{OCCH}_3$  bond, an  $\text{H}_2\text{O}$  bridge, and a peripheral  $\text{H}_2\text{O}$  molecule bonded to  $\text{CH}_3\text{COO}^-$ ; isomer B (Table 4) of  $\text{CH}_3\text{COO}^- (\text{CH}_3\text{COOH})(\text{H}_2\text{O})_2$  with an  $\text{H}_2\text{O}$  bridge and a peripheral  $\text{H}_2\text{O}$  molecule bonded to  $\text{CH}_3\text{COO}^-$ ; isomer C (Table 4) of  $\text{CH}_3\text{COO}^- (\text{CH}_3\text{COOH})(\text{H}_2\text{O})_2$  with a direct  $\text{CH}_3\text{COO}^- \cdots \text{HOOCCH}_3$  bond, a bridging  $\text{H}_2\text{O}$  molecule, and a peripheral bridging  $\text{H}_2\text{O}$  molecule bonded to  $\text{CH}_3\text{COO}^-$  and to the bridging  $\text{H}_2\text{O}$  molecule; and isomer D (Table 4) of  $\text{CH}_3\text{COO}^- (\text{CH}_3\text{COOH})(\text{H}_2\text{O})_2$  with a bridging  $\text{H}_2\text{O}$  molecule and a peripheral bridging  $\text{H}_2\text{O}$  molecule bonded to  $\text{CH}_3\text{COO}^-$  and to the bridging  $\text{H}_2\text{O}$  molecule. This material is available free of charge on the Internet at <http://pubs.acs.org>.

JA982173I